Communication and Cross-Regulation Between Multiple Concatenated Enzymatic Reaction Networks

Mo Sun,[a,c] Jie Deng,[b,d] and Andreas Walther*[b,c]

a. Present address: Department of Chemistry, Fudan University, Shanghai 200438, China

b. A^{3}BMS Lab, Department of Chemistry, University of Mainz, Duesbergweg 10-14, 55128 Mainz, Germany.

c. Cluster of Excellence livMatS @ FIT – Freiburg Center for Interactive Materials and Bioinspired Technologies, University of Freiburg, Georges-Köhler-Allee 105, 79110 Freiburg, Germany

d. Present address: Dana-Farber Cancer Institute, Wyss Institute for Biologically Inspired Engineering, Harvard Medical School, Boston, MA 02115, USA

ABSTRACT: Nature connects multiple fuel-driven chemical/enzymatic reaction networks (CRNs/ERNs) via cross-regulation to hierarchically control biofunctions for a tailored adaption in complex sensory landscapes. In contrast, emerging artificial fuel-driven systems mostly focus on a single CRN and their implementation to direct self-assembly or material responses. In this work, we introduce a facile example of communication and cross-regulation among multiple DNA-based ERNs regulated by a concatenated RNA transcription regulator. For this purpose, we run two fuel-driven DNA-based ERNs by concurrent NAD^+-fueled ligation and restriction via endonucleases (REases) in parallel. ERN one allows for the dynamic steady-state formation of the promoter sequence for T7 RNA polymerase, which activates RNA transcription. The produced RNA regulator can repress or promote the second ERN via RNA-mediated strand displacement. Furthermore, adding RNase H to degrade the produced RNA can restart the reaction or tune the lag time of two ERNs, giving rise to a repression-recovery and promotion-stop processes. We believe that concatenation of multiple CRNs provides a basis for the design of more elaborate autonomous regulatory mechanisms in systems chemistry and synthetic biology.

Introduction

Man-made self-assembling system can be categorized into three main thermodynamic regimes: thermodynamic equilibrium, kinetically trapped out-of-equilibrium, and fuel-driven out-of-equilibrium.[1] Classically, synthetic system have focused on thermodynamic equilibration and kinetic traps.[2-7] However, nature organizes many structures and functions in an energy-driven way out-of-equilibrium, because this can be beneficial for a quicker adaptation in response to a signal.[8] Microtubules, designed for adaptive spatial search, are the most striking example, continuously consuming guanosine triphosphate (GTP) as the energy to maintain a dynamic steady state (DySS) between polymerization and depolymerization. The dynamics of microtubules change drastically during cell division, because the interaction of the simple cyclic microtubule reaction network with other biological signaling systems using chemicals species leads to a change in their behavior.

Although there has been significant progress in the design of chemically fueled self-assemblies using a diversity of fuels, building blocks and approaches,[9-17] one of the next challenges is to increase behavioral complexity by interfacing such systems with secondary regulatory feedback mechanisms. As in living systems, biological activity and behavior are a collection of different individual reaction networks and signaling systems, and similarly, synthetic out-of-equilibrium systems should be advanced to contain interacting reaction network modules to achieve higher regulation in the behavior. While this has been realized for chemically similar species, such as using the PEN toolbox to reach bistability or oscillatory behavior,[18-20] or RNA transcription/degradation systems, a key challenge remains to couple system with rather distinct chemistries.[21]

We set out to address this challenge of achieving interaction between two dynamic chemical systems by coupling our recently developed ATP-driven non-equilibrium DNA ligation/restriction system with an RNA transcription system to achieve cross-regulation and feedback. The ATP-driven system is based on an enzymatic reaction network (ERN) balancing fuel-driven ligation of sticky end-functionalized DNA building blocks using T4 DNA ligase with restriction at the same position using endonucleases (REases).[22] In short, the fuel (ATP) sets the lifetime of the out-of-equilibrium state, and the ratio of the enzymes engineers the dynamics of the DySS. The system is highly versatile, and we could demonstrate pathway complexity and reconfiguration using pools of species or combination of REases,[23-24] photo-activation of fuels and building blocks,[25] and translation into hierarchical assemblies.[26-27] Additionally, we could connect it to strand displacement reactions as a first communication principle between two networks of distinct thermodynamic nature.[28,29]

Herein, we introduce a connection of our ligation/restriction ERN with an RNA transcription machinery to implement new types of regulatory effects. We demonstrate cross-regulation from a primary DNA to a secondary DNA ERN by information exchange using co-transcribed RNA. The use of RNA opens the perspective to use orthogonal enzymes and chemo-specific degradation as additional control tools. We describe four modes of interference with respect to the ligation/restriction ERN: Repression, promotion, repression-recovery and promotion-stop. We believe that these additional control mechanisms can help

to promote regulatory functions, signal processing and adaptation capacity to future chemically instructed materials systems with life-like behavior.

Results and Discussion

Design

Our systems contain two ligation/restriction ERNs, (1) a template network (TemN) and (2) a report network (RepN), that are susceptible for cyclic operation by enzymes as further detailed below (Scheme 1). Both TemN and RepN share the same chemical fuel to program their transient lifecycles. The monomeric DNA building block in TemN (M_T) contains the promoter and template for RNA polymerase and is susceptible to oligomerization using a fuel-consuming ligase by covalent linkage of the sticky end. It controls the ON-OFF switch of the RNA transcription. The RNA transcription can only proceed in the ligated state, because M_T only contains a partial promoter sequence that is only transformed into the full promoter codon in the oligomerized state (O_T). The templating sequence for RNA transcription on O_T is designed to induce cross-talk with RepN via RNA-mediated strand displacement in the reporter species, M_R. Thus, RepN is used to show the chemical information exchange between TemN and RepN, including four different results, repression, promotion, repression-recovery, and promotion-stop, based on the different sequence designs and enzymes.

Let us start with repression as first example: Without RNA production (in absence of T7 RNA polymerase (T7 RNAP)), RepN forms a similar DySS as TemN. When RNA is transcribed, RNA can however transform the reactive monomer, M_R, into non-reactive monomer (M_{RN}) by strand displacement to shut down RepN. Since both TemN and RepN run on the same fuel (β-nicotinamide adenine dinucleotide, NAD^+), their cross-activated behavior influences each other's transient lifecycles with respect to the availability of the fuel NAD^+. For instance, in an activated repression process, the RepN will have a shortened lifetime as forced by the produced RNA, while concurrently, a longer lifetime of TemN should be achieved due to higher fuel availability as the competition for the fuel is lost for by the suppressed RepN (Scheme1A).

In contrast, in a promotion process, a non-reacting M_{RN} in the RepN exists at the beginning, and, only if RNA is produced, then M_{RN} transforms into M_R to start RepN. Thus, in a promotion process, the RepN will experience a lag time in the cyclic operation compared to TemN and is also fully conditional on the presence of T7 RNAP (Scheme 1B).

Higher behavioral complexity is possible by adding ribonuclease (RNase) to degrade the RNA at the same. We will elucidate that this allows to switch the repression process into a repression-recovery process, because when the produced RNA is completely degraded, M_{RN} will be transformed back to M_R to restart RepN (Scheme 1C). The addition of RNase to the promotion process leads to a promotion-stop process, wherein the lag time of two ERNs will be tuned by the RNase amount (Scheme 1D).

The cyclic DNA ligation/restriction ERNs use a ligase and two different REases, which we chose specifically to minimize unwanted crosstalk, and highlight the importance of the RNA-regulators, as well as fuel competition of both cyclic DNA ERNs. In contrast to our earlier work on ATP-driven cyclic ligation/restriction networks based on T4 DNA ligase,[21-27] we herein introduce *E. coli* DNA ligase, that is able to ligate DNA fragments with 3'-OH and 5'-phosphate ends, but uses NAD^+ instead of ATP (for T4 DNA ligase) as fuel. This prevents competition for the ATP fuel, because T7 RNAP also uses ATP during the transcription step. For the REases, we chose BsaI in TemN because BsaI shows an excellent programmability of the recognition site,[26] while EcoRI is used in RepN because it is robust and efficient.[24] The DNA-to-RNA transcription uses T7 RNAP, a DNA-dependent RNA polymerase, that is highly specific for specific promoters, using a ribonucleotide solution mix (NTP, containing ATP, UTP, GTP, CTP) as the starting reactants. RNase H is used as an RNase to specifically degrade RNA hybridized to DNA.

Scheme 1. RNA-based Feedback Regulation between Two Cyclic Ligation/Restriction Networks

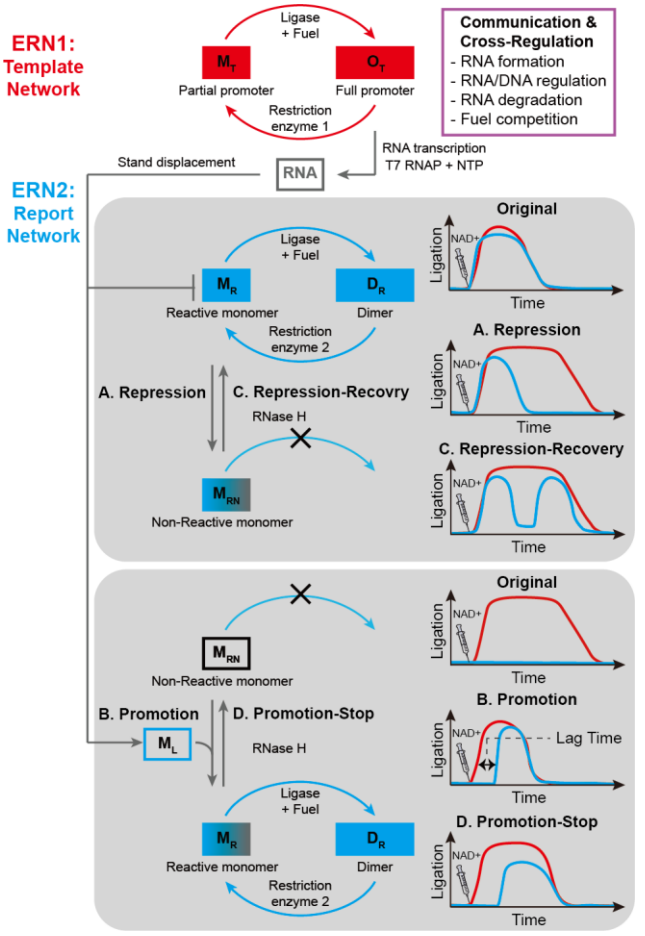

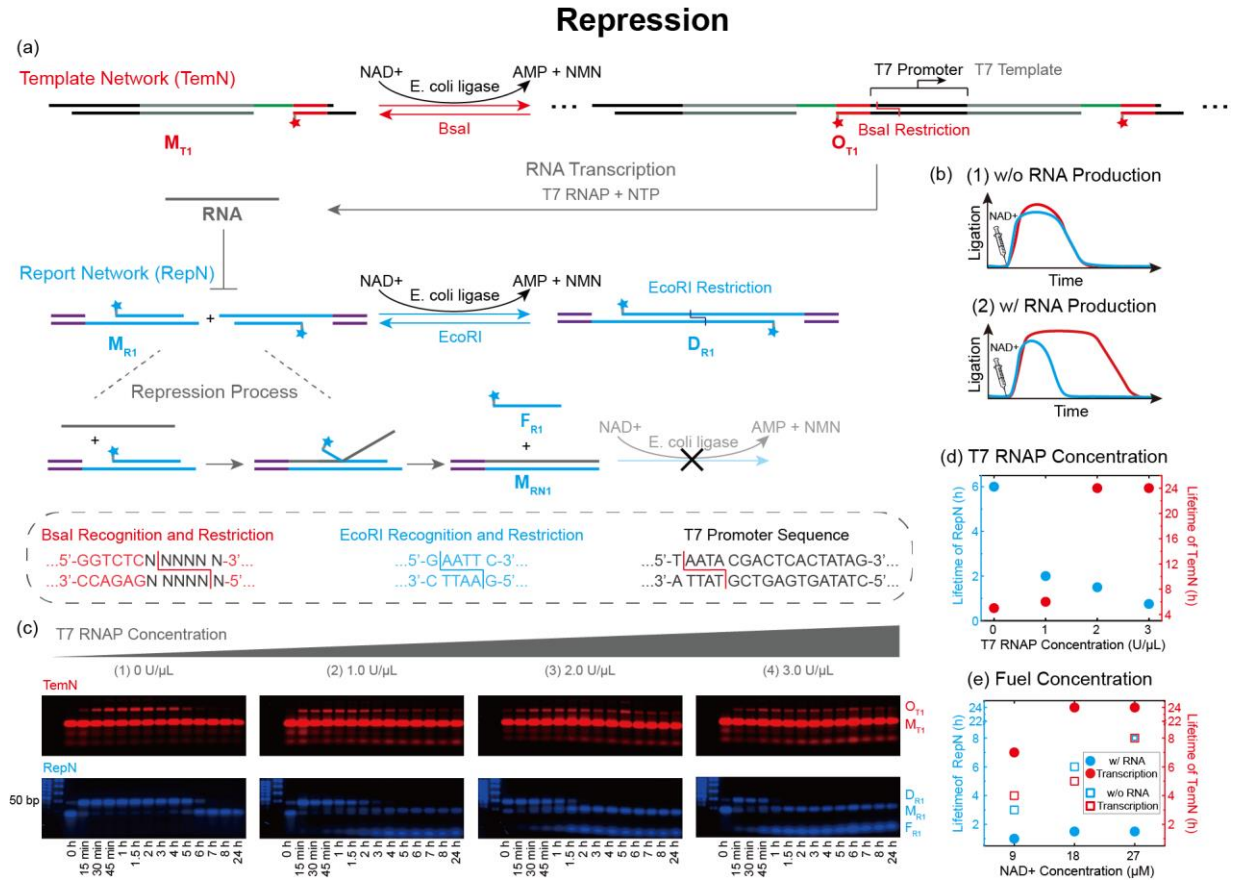

Figure 1. Repression. (a,b) Schematic illustration of the repression process between two DNA-based ERNs (AMP for adenosine monophosphate; NMN for nicotinamide mononucleotide). (c) Time-dependent transient polymerization curves and (d) lifetime analysis of the repression with [T7 RNAP]. Other conditions: 5.0 μM M_{T1}, 10.0 μM M_{R1}, 16.0 U/μL ligase, 0.67 U/μL EcoRI, 0.89 U/μL BsaI, 2.0 mM NTP, and 18.0 μM NAD^+. (e) lifetime analysis of the repression with [NAD^+]. Other conditions: 5.0 μM M_{T1}, 10.0 μM M_{R1}, 16.0 U/μL ligase, 0.67 U/μL EcoRI, 0.89 U/μL BsaI, 2.0 U/μL T7 RNAP, and 2.0 mM NTP. The minor red fluorescent bands at high migration distance correspond to some minor stochiometric imbalance.

Repression

The design and analysis of the repressive signaling loop works as follows (Figure 1a): In TemN, the Cy5-labeled DNA sequence of M_{T1} is designed to contain a BsaI recognition site (red part), a disconnected T7 promoter (black part), a T7 template (gray part), and a T7 RNAP run-off sequence (green). The ends of M_{T1} contain one 4 nucleotide (nt) sticky end 5'-AATA-3' on one side and the complementary sticky end 5'-TATT-3' on the other side (detailed DNA sequences in Table S1). In relation to our previous work on ATP-driven ERNs,[22] M_{T1} can be grown into an oligomer state O_{T1} and reaches a DySS depending on the ligase/BsaI ratio and the fuel amount (here now NAD^+ and not ATP due to the use of E. coli ligase). To achieve the fuel-dependent ON-OFF transcription, the BsaI restriction site is located within the T7 promoter −16 site, breaking the whole promoter region into two in the non-fueled ground state. However, during operation of the NAD^+-fueled cyclic ligation/restriction ERN, M_{T1} enters the oligomer state O_{T1} with the full T7 promoter sequence that encodes RNA transcription. In RepN, the fluorescein-labeled monomer (M_{R1}) is designed with a 4-nt self-complementary sticky end 5'-AATT-3' for ligation and EcoRI cutting, as well as with a segment F_{R1}, which can be removed by toehold-mediated strand displacement of the produced RNA. On its own and without considering the produced RNA, the presence of *E. coli* ligase/EcoRI and fuel NAD^+ induces a transient DySS, in which M_{R1} will form a dimer D_{R1}, that is cut back to the monomer state after consumption of the fuel. Operating these two ERNs together without T7 RNAP, that is in absence of RNA transcription and strand displacement, these two ERNs of TemN and RepN run independently. In contrast, in presence of T7 RNAP, the produced RNA will displace the fluorescein-labeled strand F_{R1} through strand displacement, yielding a non-reactive DNA-RNA hybrid monomer M_{RN1}, which lacks the sticky end for ligation. This process eventually stops the RepN. Due to the early repression of RepN, the fuel, previously shared between TemN and RepN, will be exclusively used by TemN, causing a stronger ligation and longer lifetime of TemN (Figure 1b2).

Figure 1c displays the results of this repression process with multicolor agarose gel electrophoresis (AGE) of the time-dependent transient systems of TemN and RepN with different amounts of T7 RNAP. Since M_{T1} and M_{R1} share the ligase and NAD^+ in the reaction, the kinetic balance between ligated and cut species is mainly controlled by the REases' reactivity. Thus, both color channels for the TemN (red) and the RepN (blue) show the individual transient systems, with the transient appearance of higher molecular weight species with a limited lifetime.

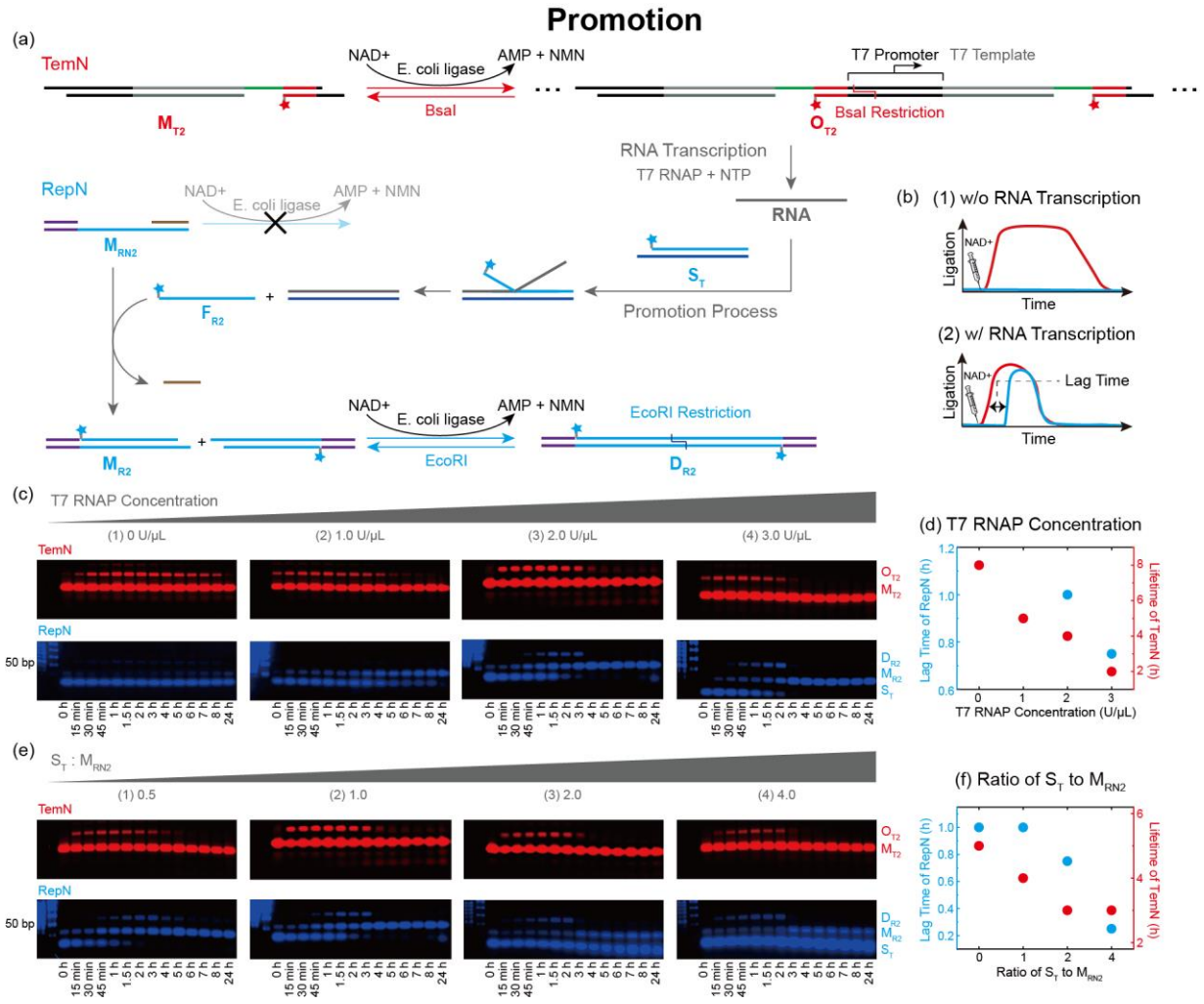

Figure 2. Promotion. (a,b) Schematic illustration of the promotion process between two ERNs. (c) Time-dependent transient polymerization curves and (d) lifetime analysis of the repression with [T7 RNAP]. Other conditions: 10.0 μM M_{T2}, 10.0 μM M_{RN2}, 10.0 μM S_T, 10.0 U/μL ligase, 0.5 U/μL EcoRI, 1.5 U/μL BsaI, 2.0 mM NTP, and 9.0 μM NAD^+. (e) Time-dependent transit polymerization curves and (f) lifetime analysis of the repression with different ratios of ST to M_{RN}. Other conditions: 10.0 μM M_{T2}, 10.0 μM M_{RN2}, 10.0 U/μL ligase, 0.5 U/μL EcoRI, 1.5 U/μL BsaI, 2.0 U/μL T7 RNAP, 2.0 mM NTP and 9.0 μM NAD^+.

In absence of T7 RNAP, meaning without RNA transcription, the lifetimes of the DySSs for the red TempN and blue RepN are very similar at about 5 h and 6 h (Figure 1c1). In the transient DySS (i.e. at 1 – 2 h), the monomeric band for M_{T1} is hardly visible, because the majority of M_{T1} is present as a dynamic dimer as first oligomeric species (O_{T1}). When adding 1.0 U/μL T7 RNAP, the RepN lifetime decreases sharply to only 2 h, whereas the TemN lifetime increases to 7 h. At the same time, a new band corresponding to F_{R1} appears in AGE after 1.5 h, which originates from the RNA-induced strand displacement of F_{R1} from M_{R1}. Concurrently, the unreactive M_{RN1} is formed. By further increasing [T7 RNAP] to 2.0 U/μL and 3.0 U/μL, the TemN lifetimes increase to as long as 24 h, and the RepN lifetimes shorten to 1.5 h and 45 min (Figures 1c3,4 and 1d). Concurrently, the F_{R1} band appears earlier and more pronounced, because the more T7 RNAP, the faster is RNA transcription and the faster is the formation of M_{RN1}.

It should be noticed that the addition of T7 RNAP, besides changing the lifetimes, also increases the ligation ratio of TemN in the DySS because more NAD^+ fuel is available for the TemN due to repression of RepN. This is shown in Figure S1, where the oligomerization of M_{T1} proceeds to clearly longer oligomers after adding 2.0 U/μL T7 RNAP. Note that for simplicity, we only show the monomer/dimer part of the AGE here.

To underscore the general tuneability of the system, the Supporting Information depicts related experiments for different [NAD^+] (Figures 1e, S2), as well as for different [NTP] (Figure S3). More NAD^+ increases the lifetimes of both TemN and RepN and less NTPs weaken the repression due to fewer and slower RNA production.

Promotion

To achieve the promotion process, we slightly modified the M_{T1} structure to M_{T2} to fit to the newly needed TemN/RepN combination. The building block in RepN is completely redesigned into an unreactive monomer, M_{RN2}, in which the reactive, self-complementary sticky ends for ligation are shielded by short complementary strands (brown). Additionally, a signal transducer, S_T, is present (Figure 2a), that can convert the generated RNA into an output activating M_{RN2} by strand displacement of the short, brown shielding strand. The translated signal carries a fluorescent dye, so that its transfer into the activated monomer M_{R2} and subsequent dimerization in the cyclic ERN can be visualized. If there is no transcription, only TemN runs

as a fuel-driven ERN (Figure 2b1). If the transcription is switched on, the M_{R2} generated by downstream strand displacement of M_{RN2} via the produced RNA enters the cyclic ligation/restriction ERN in RepN. This delayed activation of RepN concurrently is expected to reduce the lifetime of TemN compared to no transcription conditions due to competition for the NAD^+ fuel for the ligase.

We first investigated the effect of [T7 RNAP] on this promotion process (Figures 2c,d). In absence of T7 RNAP, the lifetime of TemN is over 8 h (red channel), and a major single fluorescent band is visible in the blue channel corresponding to intact S_T (note that some minor unavoidable leakage happens). When gradually increasing [T7 RNAP] from 1.0 to 3.0 U/µL, the RepN becomes continuously activated. At 1.0 U/µL the band corresponding to the activated monomer M_{R2} clearly forms, but a dimerization is hardly visible (blue channel; Figure S4). Clear dimerization occurs for higher [T7 RNAP], which leads to sufficient RNA production for a complete signal conversion from S_T to M_{R2} and ensuing dimerization. The lag times decrease from 45 min (2.0 U/µL T7 RNAP) to 30 min (3.0 U/µL T7 RNAP), but clearly there are kinetic delays due to the need for signal translation. Concurrently, the lifetimes of TemN decrease from 5 - 2 h, and the lifetimes of the RepN synchronize, because the same stop time is set when the fuel NAD^+ in the solution is used up.

Considering S_T and M_{RN2} to be the key components in this promotion process, we studied the influence of their ratio (Figures 2e,f). At the same concentration of M_{T2} and M_{RN2} (10.0 µM), the lifetimes of TemN decrease from 5 - 3 h when increasing [S_T] from 10.0 to 40.0 µM (ratio of S_T to M_{RN2} from 1.0 to 4.0), because more reactive M_{R2} is produced and RepN consumes more fuels. Also, the lag time shortens from 45 min to 15 min when increasing [S_T] to 40.0 µM. This is due to the fact that a higher [S_T] will accelerate the strand displacement reaction rate and thus gives a faster formation of M_{R2}

Repression-Recovery and Promotion-Stop

As next step, we introduce RNase H, an endoribonuclease that specifically hydrolyzes RNA phosphodiester bonds in DNA-RNA hybrids to degrade RNA strands. The addition of this RNA sink now evolves the system towards a combination of two kinds of ERNs: one cyclic ligation/restriction ERN running on NAD^+ (to steer TemN and RepN), and one non-cyclic ERN working as an RNA production/degradation scheme running on NTPs. We hypothesized that this would allow more elaborate temporal control in the autonomous systems, as for instance the RNA-induced intermediate M_{RN1} (unreactive in RepN) could be forced to be regenerated to the reactive M_{R1} to push the previously stopped RepN back to an active state (Figure 3a). We call this process “Repression-Recovery”. Experimentally, we added a large amount of NAD^+ (36.0 µM) to maintain TemN operational for long times during the experiments and to allow a focus on the repressed RepN. [RNase H] was varied from very low (0.011 U/µL) to moderate (0.039 U/µL) and high concentrations (0.11 U/µL; Figure 3b). Indeed, [RNase H] shows a profound influence. Three regimes can be distinguished. At very low [RNase H] of 0.011 U/µL, the behavior is qualitatively similar to systems without RNase H. The repression works effectively and the intermediately formed D_{R2} is effectively suppressed by the upstream RNA production (after 1 h). The fluorescent F_{R1} band (indicative of efficient RNA-mediated strand displacement) appears thereafter and exists for a long time (Figure 3b1). The RNase H cannot provide a fast-enough digestion of the RNA in M_{RN1} to allow for reactivation of the RepN to the D_{R2} reporter. After 24 h, different from the repression process, the F_{R1} band disappears and M_{R1} reappears. This confirms that RNase H digests the RNA bound to M_{RN1}, yet in a too slow manner to be relevant for the transient system.

In presence of moderate [RNase H] of 0.039 U/µL, a repression-recovery process appears (Figure 3b2). From 15 min to 5 h, the first round of a typical repression process occurs, with the D_{R1} band appearing at 15 min and disappearing at 2 h. The F_{R1} band appears at 45 min. However, after 5 h, the F_{R1} band gradually weakens and the D_{R1} band reappears, indicating substantial RNA degradation and reengagement of the reformed M_{R1} into the RepN. At 24 h, no F_{R1} remains, and only M_{R1} is left according to AGE, and the system returns to the initial state. The appearance of the two states can be explained by the fact that the RNA is generated quickly to take effect in the RepN, but then degraded on a system-relevant time scale.

The third situation can be induced upon addition of large quantities of RNase H of 0.11 U/µL (Figure 3b3). At this point, the hydrolysis rate of RNA by RNase H is so fast that the RNA-induced reconfiguration of reactive M_{R1} into M_{RN1} does not occur. There is hardly any band for F_{R1} visible, which is the strongest proof of a speedy recovery of M_{R1} from M_{RN1}. Note that RNase H is selective to RNA degradation on DNA. Consequently, RepN runs similarly as TemN until the fuel has run out.

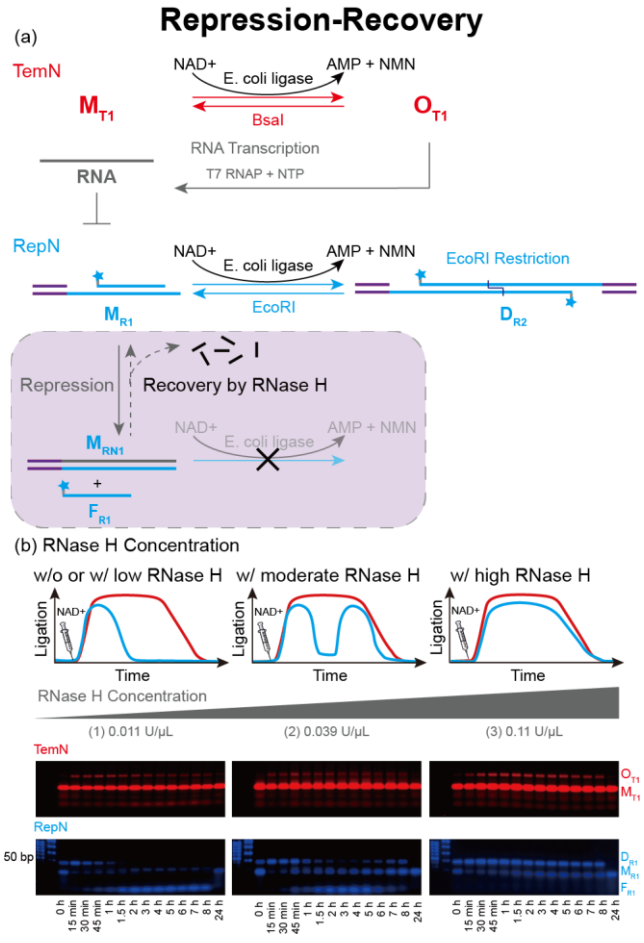

Figure 3. Repression-Recovery. (a) Schematic illustration of the repression-recovery process between two ERNs. (b) Time-dependent transient polymerization curves the repression-recovery with [RNase H]. Other conditions: 5.0 µM M_{T1}, 10.0 µM M_{R1}, 16.0 U/µL

ligase, 0.67 U/μL EcoRI, 0.89 U/μL BsaI, 2.0 U/μL T7 RNAP, 2.0 mM NTP, and 36.0 μM NAD^+.

At last, we introduce the RNase H into the promotion process that works based on the signal transducer S_T to recode the RNA information for more elaborate control over the signal transducing events. Figure 4a displays that the addition of the RNase H can recover the intermediate S_I to S_T. Indeed upon increasing [RNAse H] from 0.011 U/μL, 0.028 U/μL to 0.05 U/μL, the lag times in RepN increase from 30 min to infinity, as more S_T remains present in the solution. Since high RNase H concentrations suppress efficient downstream activity of the produced RNA strand into the RepN, the TemN shows a longer lifetime from 4 h to 5 h and 6 h, because less M_{R2} is generated and more NAD^+ fuel is available to TemN (Figure 4b).

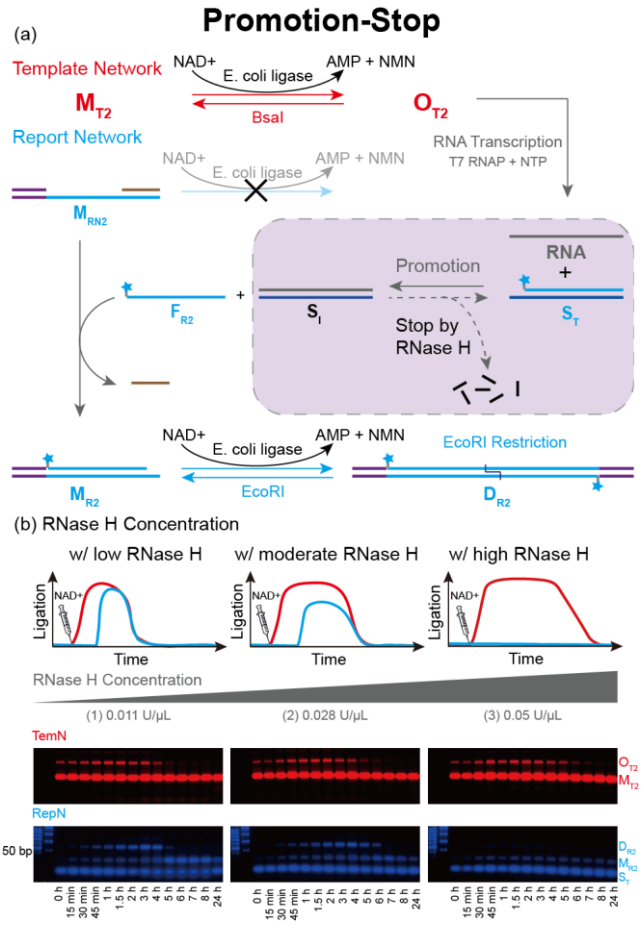

Figure 4. Promotion-Stop. (a) Schematic illustration of the promotion-stop process between two ERNs. (b) Time-dependent transient polymerization curves the repression-recovery with [RNase H]. Other conditions: 10.0 μM M_{T2}, 10.0 μM M_{RN2}, 10.0 μM S_T, 10.0 U/μL ligase, 0.5 U/μL EcoRI, 1.5 U/μL BsaI, 2.0 U/μL T7 RNAP, 2.0 mM NTP, and 18.0 μM NAD^+.

Conclusion

In summary, we introduced versatile strategies for the cross-regulation of two out-of-equilibrium ERNs yielding four different types of behavior (repression, promotion, repression-recovery, and promotion-stop) by on-demand integration of RNA transcription and degradation machinery. The communication occurs by conditional information exchange or RNA and RNA-mediated strand displacement reactions. The fuel-driven formation of T7 promoter sequence in TemN is a key factor to initiate the cross-talk, as otherwise two independent ERN-based DySSs occur. The T7 RNAP concentration governs the RNA transcription rate and thereby the strength of communication, which effectively controls the lifecycles of both concatenated TemN and RepN. A secondary cross-regulation occurs, because the NAD^+ fuel, originally shared equally between TemN and RepN, becomes unequally shared. This influences the lifetimes and the fractional degrees of ligation in TemN and RepN. Adding a sink for the RNA messenger via RNase H allows to reach additional behavioral modes. In future, it will be important to develop full kinetic models allowing for a predictive behavior,[26] but at this point too many of the kinetic parameters, in particular on the NAD^+-driven ERNs, are still unknown and require substantial efforts to be obtained.

In a wider perspective of systems chemistry, this work adds another layer of complexity compared to typically operated individual cyclic reaction networks[10,14,30] which are important for the design of autonomous systems and more intelligent materials. Even though biological machinery and enzymes are robust tools for the implementation of such a communication and cross-regulation behavior, we believe that the guidelines provided here are also relevant to improve fully man-made regulatory networks in supramolecular chemistry, or even classic polymer chemistry.

ASSOCIATED CONTENT

Supporting Information. Details of experimental and some gel electrophoresis data are listed in Supporting Information. This material is available free of charge via the Internet at http://pubs.acs.org.

AUTHOR INFORMATION

Corresponding Author

*Andreas Walther. Email: andreas.walther@uni-mainz.de

Notes

The authors declare no competing interests.

ACKNOWLEDGMENT

The authors acknowledge support by the European Research Council starting Grant (TimeProSAMat). This work was funded by the Deutsche Forschungsgemeinschaft (DFG, German Research Foundation) under Germany's Excellence Strategy – EXC-2193/1 – 390951807 via "Living, Adaptive and Energy-Autonomous Materials Systems" (livMatS).

REFERENCES

1. Mattia, E.; Otto, S. Supramolecular Systems Chemistry. *Nat. Nanotechnol.* **2015,** *10* (2), 111-119.
2. Levin, A.; Hakala, T. A.; Schnaider, L.; Bernardes, G. J. L.; Gazit, E.; Knowles, T. P. J. Biomimetic Ppeptide Self-Assembly for Functional Materials. *Nat. Rev. Chem.* **2020,** *4* (11), 615-634.
3. Shen, B.; Kim, Y.; Lee, M. Supramolecular Chiral 2D Materials and Emerging Functions. *Adv Mater* **2020,** *32* (41), 1905669.
4. Liu, Y.; Chen, Y.; Zhang, H.-Y., *Handbook of Macrocyclic Supramolecular Assembly*. Springer Singapore: 2019.
5. Lu, Y.; Lin, J.; Wang, L.; Zhang, L.; Cai, C. Self-Assembly of Copolymer Micelles: Higher-Level Assembly for Constructing Hierarchical Structure. *Chem. Rev.* **2020,** *120* (9), 4111-4140.
6. Gao, C.; Chen, G. Exploring and Controlling the Polymorphism in Supramolecular Assemblies of Carbohydrates and Proteins. *Acc. Chem. Res.* **2020,** *53* (4), 740-751.

7. Sun, M.; Lee, M. Switchable Aromatic Nanopore Structures: Functions and Applications. *Acc. Chem. Res.* **2021,** *54* (14), 2959-2968.

8. Walther, A. Viewpoint: From Responsive to Adaptive and Interactive Materials and Materials Systems: A Roadmap. *Adv. Mater.* **2020,** *32* (20), 1905111.

9. Del Grosso, E.; Prins, L. J.; Ricci, F. Transient DNA-Based Nanostructures Controlled by Redox Inputs. *Angew. Chem. Int. Ed.* **2020,** *59* (32), 13238-13245.

10. Deng, J.; Walther, A. ATP-Responsive and ATP-Fueled Self-Assembling Systems and Materials. *Adv. Mater.* **2020,** *32* (42), e2002629.

11. Singh, N.; Formon, G. J. M.; De Piccoli, S.; Hermans, T. M. Devising Synthetic Reaction Cycles for Dissipative Nonequilibrium Self-Assembly. *Adv. Mater.* **2020,** *32* (20), 1906834.

12. van Esch, J. H.; Klajn, R.; Otto, S. Chemical Systems Out of Equilibrium. *Chem. Soc. Rev.* **2017,** *46* (18), 5474-5475.

13. Hwang, I.; Mukhopadhyay, R. D.; Dhasaiyan, P.; Choi, S.; Kim, S. Y.; Ko, Y. H.; Baek, K.; Kim, K. Audible Sound-Controlled Spatiotemporal Patterns in Out-of-Equilibrium Systems. *Nat. Chem.* **2020,** *12* (9), 808-813.

14. Rieß, B.; Grötsch, R. K.; Boekhoven, J. The Design of Dissipative Molecular Assemblies Driven by Chemical Reaction Cycles. *Chem* **2020,** *6* (3), 552-578.

15. Del Grosso, E.; Ponzo, I.; Ragazzon, G.; Prins, L. J.; Ricci, F. Disulfide-Linked Allosteric Modulators for Multi-cycle Kinetic Control of DNA-Based Nanodevices. *Angew. Chem. Int. Ed.* **2020,** *59* (47), 21058-21063.

16. Heinen, L.; Walther, A. Celebrating Soft Matter's 10th Anniversary: Approaches to program the time domain of self-assemblies. *Soft Matter* **2015,** *11* (40), 7857-7866.

17. Zhou, Z.; Ouyang, Y.; Wang, J.; Willner, I. Dissipative Gated and Cascaded DNA Networks. *J. Am. Chem. Soc.* **2021,** *143* (13), 5071-5079.

18. Baccouche, A.; Montagne, K.; Padirac, A.; Fujii, T.; Rondelez, Y. Dynamic DNA-Toolbox Reaction Circuits: a Walkthrough. *Methods* **2014,** *67* (2), 234-249.

19. Schaffter, S. W.; Schulman, R. Building in vitro Transcriptional Regulatory Networks by Successively Integrating Multiple Functional Circuit Modules. *Nat. Chem.* **2019,** *11* (9), 829-838.

20. Green, L. N.; Subramanian, H. K. K.; Mardanlou, V.; Kim, J.; Hariadi, R. F.; Franco, E. Autonomous Dynamic Control of DNA Nanostructure Self-Assembly. *Nat. Chem.* **2019,** *11* (6), 510-520.

21. Deng, J.; Walther, A. Fuel-Driven Transient DNA Strand Displacement Circuitry with Self-Resetting Function. *J. Am. Chem. Soc.* **2020,** *142* (50), 21102-21109.

22. Heinen, L.; Walther, A. Programmable Dynamic Steady States in ATP-Driven Nonequilibrium DNA Systems. *Sci. Adv.* **2019,** *5* (7), eaaw0590.

23. Deng, J.; Walther, A. Pathway Complexity in Fuel-Driven DNA Nanostructures with Autonomous Reconfiguration of Multiple Dynamic Steady States. *J. Am. Chem. Soc.* **2020,** *142* (2), 685-689.

24. Sun, M.; Deng, J.; Walther, A. Polymer Transformers: Interdigitating Reaction Networks of Fueled Monomer Species to Reconfigure Functional Polymer States. *Angew. Chem. Int. Ed.* **2020,** *59* (41), 18161-18165.

25. Deng, J.; Bezold, D.; Jessen, H. J.; Walther, A. Multiple Light Control Mechanisms in ATP-Fueled Non-equilibrium DNA Systems. *Angew. Chem. Int. Ed.* **2020,** *59* (29), 12084-12092.

26. Deng, J.; Walther, A. ATP-Powered Molecular Recognition to Engineer Transient Multivalency and Self-Sorting 4D Hierarchical Systems. *Nat. Commun.* **2020,** *11*, 3658.

27. Deng, J.; Walther, A. Programmable ATP-Fueled DNA Coacervates by Transient Liquid-Liquid Phase Separation. *Chem* **2020,** *6* (12), 3329-3343.

28. Deng, J.; Walther, A. Autonomous DNA Nanostructures Instructed by Hierarchically Concatenated Chemical Reaction Networks. *Nat. Commun.* **2021,** *12*, 5132.

29. Heckel, J.; Batti, F.; Mathers, R. T.; Walther, A. Spinodal Decomposition of Chemically Fueled Polymer Solutions. *Soft Matter* **2021,** *17* (21), 5401-5409.

30. Das, K.; Gabrielli, L.; Prins, L. J. Chemically Fueled Self-Assembly in Biology and Chemistry. *Angew. Chem. Int. Ed.* **2021,** *60* (37), 20120-20143.

Table of Contents